Heat-capacity study of nematic-isotropic and nematic–smectic-A transitions for octylcyanobiphenyl in silica aerogels

L. Wu,* B. Zhou, and C. W. Garland
Department of Chemistry and Center for Material Science and Engineering, Massachusetts Institute of Technology, Cambridge, Massachusetts 02139

T. Bellini
Dipartimento di Elettronica, Università di Pavia, 27100 Pavia, Italy

D. W. Schaefer
Sandia National Laboratories, Albuquerque, New Mexico 87185
(Received 20 July 1994)

Quenched randomness and finite size can both have substantial effects on critical behavior at phase transitions. A high-resolution ac calorimeter study has been carried out on octylcyanobiphenyl (8CB) in four silica aerogels of different porosities (mass densities $\rho=0.08-0.60$ g cm^{-3}). The weakly-first-order nematic-isotropic (N-I) and second-order nematic–smectic-A (N–Sm-A) transitions in bulk liquid crystals belong to different universality classes and have been very well characterized in bulk 8CB. The excess heat capacity peaks $\Delta C_p(N\text{-}I)$ and $\Delta C_p(N\text{–Sm-}A)$ are observed to undergo distinctly different changes as a function of aerogel density. The changes in peak height $h\equiv\Delta C_p(\max)$ and peak position $T_{\rm peak}$ relative to the bulk values are not well represented by finite-size scaling for either transition, and the underlying influence of quenched randomness is discussed as the major cause of the observed effects.

PACS number(s): 64.70.Md, 61.30.−v, 82.70.Rr

I. INTRODUCTION

The effects of quenched disorder and finite size on critical behavior at phase transitions in fluid systems is a topic of considerable current interest. During the past few years, light scattering and heat capacity studies have been carried out on high-porosity silica aerogels containing simple fluids near their liquid-gas critical points [1,2], critical binary liquid mixtures [3], and ^{4}He and ^{3}He-^{4}He mixtures near the normal-superfluid transition [4,5]. Bulk liquid crystals represent fluids that exhibit a considerable variety of orientational and translational ordering transitions, and quite recently there have been heat capacity [6], light scattering [6,7], and x-ray scattering [8] studies of octylcyanobiphenyl (8CB) in silica aerogels with an average pore size of about 200 Å. Additional calorimetric work on liquid crystals confined in porous glasses with well-defined cylindrical cavities [9–11] has also shown that pore size and wall effects can have a substantial effect on liquid crystal ordering. In the case of aerogels, liquid crystal transitions should be strongly influenced by the random structure. It has been predicted that this will make the nematic (N)-isotropic (I) phase behavior analogous to that of a random-field Lebwohl-Lasher model [12,13] and the nematic–smectic-A (Sm-A) transition may become a spin-glass-like transition [12].

The present investigation involves a detailed calorimetric study of 8CB in a series of four base-catalyzed aerogels of differing porosities. Such aerogels consist of a random network of silica backbones in an openly connected void space. Small-angle x-ray scattering (SAXS) has shown that these aerogels are fractal over a limited range in length scale [14–17]. A fractal dimension of 2.0 ± 0.2 is revealed directly in the scattering profile (Porod behavior) for very low density aerogels [14] and is implicit in the measured density dependence of the pore size for the entire series studied here [17]. SAXS also shows that the silica backbones are smooth over length scales between 10 and 50 Å. Aerogels of this type are often called "colloidal" [14].

The bulk liquid crystal 8CB undergoes two phase transitions: a weakly first-order N-I orientational ordering transition at $T_{NI}^{\rm bulk}$ and a second-order N–Sm-A translational ordering transition at $T_{NA}^{\rm bulk}\simeq T_{NI}^{\rm bulk}-7$ K. For the bulk N-I transition the order parameter is a 3×3 symmetric traceless tensor with $n=5$ independent components, the so-called Q model of Priest and Lubensky [18] which describes fluctuations near $T_{NI}^{\rm bulk}$. In the mean-field approximation, rotational invariance allows the order parameter to be taken as diagonal and one obtains the Lebwohl-Lasher [19] or the Maier-Saupe [20] model. Since the free energy has cubic invariants, the N-I transition is first order, but significant energy fluctuations occur in the isotropic phase of 8CB, as indicated by high-resolution heat capacity data [21,22]. The bulk N–Sm-A transition belongs to the three-dimensional (3D) XY universality class, but the critical behavior is complicated by coupling of the smectic order parameter

*Present address: General Atomics, P.O. Box 85608, San Diego, CA 92186.

to the nematic order parameter and to director fluctuations. The effective N–Sm-A critical exponent α for the bulk heat capacity singularity in 8CB is 0.3 [21,22], representing crossover between XY and tricritical behavior. Thus a study of 8CB in aerogels allows one to characterize random-field effects on two distinctly different types of liquid crystal phase transition.

II. EXPERIMENTAL PROCEDURES AND RESULTS

The four aerogels used in this investigation were prepared by base-catalyzed polymerization of tetramethylorthosilicate in methanol to yield a network structure with strut dimensions of the order of 100 Å and internetwork voids (pores) whose average dimensions vary from 120 to 700 Å depending on the concentration of the solution precursor and the degree of collapse during drying. All the wet gels were supercritically dried, albeit the highest density sample was partially air dried (xerogelled) prior to final supercritical extraction. The two low density aerogels were obtained from Airglass AB in Sweden and the two highest density samples were synthesized at Lawrence Livermore National Laboratory by Tillotson and Hrubesh [23].

The parameters characterizing each aerogel have been determined by SAXS and are given in Table I. The silica backbones are described by an average solid chord d_s and a solid density ρ_s. The void space is described by an average pore chord $L=\langle d_p \rangle$, which represents the mean free path in the empty regions of the aerogel [17]. The pore volume fraction ϕ_p, which is given by $\phi_p = L/d$, where d is the sum chord ($d = L + d_s$), specifies the fraction of the aerogel that is available to be filled with the liquid crystal. Both L and d_s can be obtained from SAXS data with an analysis independent of phase geometry [17]. In addition to L, the distribution $g(d_p)$ or pore chords is also of interest, but more difficult to characterize. Small-angle neutron scattering studies [16] on a similar material with $\phi_p = 0.95$ confirm a fractal network structure with a measured volume fractal dimension of 2.1 and a broad distribution of void spaces ranging from 20 to 2000 Å.

The heat capacity measurements were made with a high-resolution ac calorimeter described elsewhere [24]. An input power of the form $P_0 e^{i\omega t}$ causes an oscillatory temperature response $\Delta T_{ac} e^{i(\omega t+\varphi)}$ for the sample. The magnitude ΔT_{ac} determines C_p and φ is the phase shift of the ac temperature oscillation with respect to the input power signal. This technique measures C_p rather than enthalpy, so quantitative values of latent heats at first-order transitions cannot be determined. However, there is a useful qualitative indication of two-phase coexistence in the behavior of $\tan\varphi$. At a second-order transition, $\tan\varphi$ goes through a minimum when C_p achieves its maximum value. When two phases coexist at a first-order transition, even a weakly first-order one such as the N-I transition in bulk liquid crystals, the values of $\tan\varphi$ show a pronounced increase [24,25].

TABLE I. Aerogel parameters determined from SAXS studies. ρ is the density of the gel and ρ_s is the density of the silica particles (bulk SiO_2 has a density of 2.2 g cm^{-3}). L is the average pore chord and d_s is the average solid chord. ϕ_p is the volume fraction of pores in the gel.

ρ (g cm^{-3})	L (Å)	d_s (Å)	ρ_s (g cm^{-3})	ϕ_p
0.08	700±100	42	1.48	0.945
0.17	430±65	50	1.59	0.90
0.36	180±45	47	1.73	0.79
0.60	120±25	45	2.2	0.73

Heat capacity data on bulk 8CB obtained previously with an ac calorimeter [21] are in excellent agreement with data obtained previously with a high-resolution adiabatic scanning calorimeter [22]. The transition temperatures of bulk 8CB depend slightly on the synthetic batch of 8CB obtained from BDH Chemicals but are stable over long periods. For our material, the bulk 8CB transition temperatures were determined to be $T_{NI}^{\text{bulk}} = 313.47$ K and $T_{NA}^{\text{bulk}} = 306.56$ K, in reasonably good agreement with the values of 313.88 and 306.69 K cited in Ref. [21] and 313.92 and 306.92 K cited in Ref. [22].

The specific heat C_p, i.e., heat capacity per gram of liquid crystal, is determined from

$$C_p = \frac{C_p(\text{obs}) - C_p(\text{empty cell} + \text{gel})}{m} , \tag{1}$$

where m is the mass of liquid crystal (typically 50 mg) and the heat capacity of the cell containing the empty aerogel is essentially constant over the ~30 K range of the present measurements. The filled aerogel samples were prepared in vacuum by heating 8CB into the nematic phase and allowing a 1-mm-thick slab of aerogel to fill by capillary action. This very slow and gentle filling leaves the aerogel structure intact and does not create any empty pockets that can be seen on visual inspection when the 8CB is in the isotropic phase (also confirmed by light scattering studies of identically prepared 8CB-aerogel samples [6]). Before sealing the filling aerogel into the silver cell, its surface was lightly dried with filter paper to reduce superficial excess bulk material.

Typical results are shown in Fig. 1, which compares C_p for 8CB in the $\rho = 0.17$ g cm^{-3} aerogel with C_p data for bulk 8CB [22]. Note that the 8CB background heat capacity due to noncritical contributions (given by the dashed lines) is linear in T and almost constant. Note also the very sharp C_p spike above the main N-I peak in the aerogel and another extremely weak but sharp spike near the very broad N–Sm-A aerogel peak. These spikes represent very small surface excesses of bulk 8CB. They can be eliminated by additional surface drying with filter paper and restored by adding back a very small amount of 8CB. Since it was very difficult to remove all the surface excess without also depleting some of the 8CB in aerogel pores, we chose to measure completely filled aerogels with a trace of surface excess. This strategy has the additional advantage of providing an internal reference for the bulk transition temperatures of our 8CB sample. The temperatures of these spikes in all four aerogels are 313.48±0.05 and 306.65±0.06 K, values that compare well with the independently measured transition tempera-

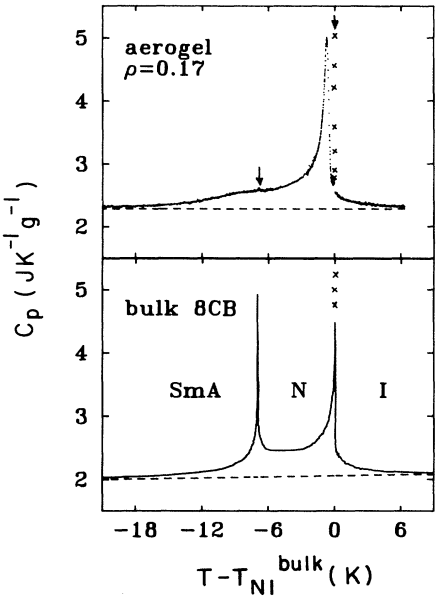

FIG. 1. Comparison between heat capacity of 8CB in a silica aerogel with density $\rho=0.17$ g cm^{-3} and that for bulk 8CB [22]. T_{NI}^{bulk} denotes the N-I transition temperature in bulk 8CB. The arrows in the top panel mark sharp C_p spikes due to a very small amount of bulk liquid crystal on the surface of the aerogel (see text). Points denoted by $\times$ are artificial C_p(coex) values obtained in a two-phase N-I coexistence region.

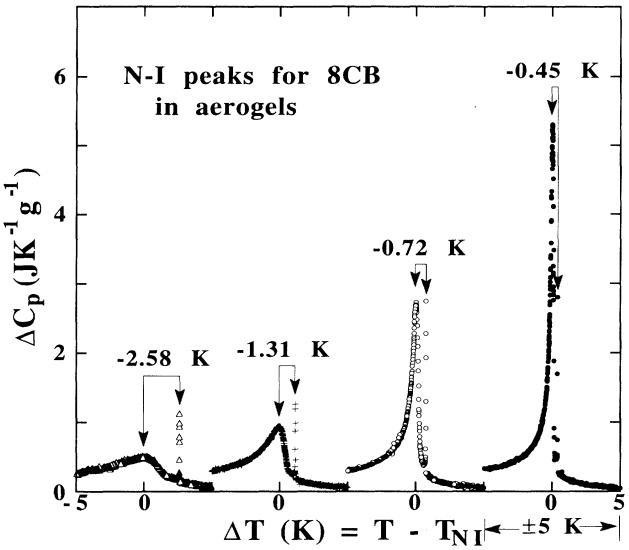

FIG. 2. Excess heat capacity for 8CB in the vicinity of the N-I transition for our aerogels. The aerogel density ρ in g cm^3 units is $\rho=0.08$ (●), 0.17 (○), 0.36 (+), and 0.60 (△). The size of the shift in the position of the N-I aerogel peak relative to the sharp spike due to N-I coexistence of the first-order transition in traces of bulk 8CB on the surface of the gel is indicated.

tures $T_{NI}^{\text{bulk}}=313.47\pm0.02$ K and $T_{NA}^{\text{bulk}}=306.56\pm0.05$ K for our batch of bulk 8CB. The N-I spike is much more prominent than the N–Sm-A spike since the bulk N-I transition is first order and apparent C_p values in a two-phase coexistence region are anomalously large [24,25]. It should be stressed that bulk 8CB has a substantial discontinuous latent heat $\Delta H=2.10$ J g^{-1} at the N-I transition in addition to the integrated pretransitional N-I enthalpy $\delta H_{NI}=5.58$ J g^{-1} and the second-order integrated N–Sm-A enthalpy $\delta H_{NA}=0.77$ J g^{-1} [21,22]. We estimate that the surface excess of bulk 8CB comprises 2–4 w% of the total 8CB in our aerogel samples, and no attempt will be made to partition the observed specific heat between a surface bulk contribution and a contribution due to 8CB in the pores of the aerogel except for the obvious suppression of surface spikes in the analysis and discussion given in Sec. III.

We shall be concerned here with the excess heat capacity ΔC_p associated with the phase transitions

$$\Delta C_p = C_p - C_p(\text{background}) . \tag{2}$$

In the vicinity of T_{NI} this quantity is completely due to configurational energy effects associated with nematic ordering and $\Delta C_p(N\text{-}I)$ peaks are shown over a ±5 K range for all four aerogels in Fig. 2. As the aerogel density ρ increases, there is a dramatic reduction in the magnitude of $\Delta C_p(N\text{-}I)$ and a systematic shift in the peak position relative to the surface spike. Note that the maximum value of $\Delta C_p(N\text{-}I)$ is greater for aerogels with $\rho=0.08$ and 0.17 than the maximum value shown for bulk 8CB in Fig. 1. However, it must be kept in mind that a δ function corresponding to the latent heat at this first-order N-I bulk transition is represented in Fig. 1 only by the three C_p(coex) points at T_{NI}^{bulk}. Although the $\Delta C_p(N\text{-}I)$ aerogel data vary smoothly throughout the peak region, the phase shift φ provides evidence of two-phase N-I coexistence for the aerogels with $\rho=0.08$ and 0.17. This is illustrated by a comparison in Fig. 3 of the tanφ temperature dependence for aerogels with $\rho=0.08$ and 0.36. The arrows indicate the location of the aerogel $\Delta C_p(N\text{-}I)$ maximum and the surface spike. For both samples, there is an extremely sharp anomaly in tanφ associated with two-phase N-I coexistence in the excess bulk 8CB on the surface. For the $\rho=0.36$ sample there is a smooth minimum in tanφ at the aerogel N-I transition temperature just like one would observe at any second-order transition or supercritical evolution in a bulk sample, whereas the $\rho=0.08$ aerogel exhibits a substantial tanφ peak at T_{NI} preceded by a dip in tanφ both above and below T_{NI}. The latter behavior is characteristic of weakly first-order transitions with substantial pretransitional fluctuation effects [25]. The tanφ behaviors of aerogels with $\rho=0.60$ and 0.17 are similar to those shown for $\rho=0.36$ and 0.08, respectively, but the temperature variations are smaller, which is expected since the $\Delta C_p(N\text{-}I)$ peaks are smaller. On the basis of tanφ data, we estimate that coexistence of N and I phases persists over a range of 0.30–0.33 K for the aerogels with $\rho=0.08$ and 0.17, but no evidence of first-order N-I coexistence is seen for aerogels with $\rho=0.36$ and 0.60. As a result of the broad N-I coexistence region in the low density aerogels, $\Delta C_p(N\text{-}I)$ is anomalously large for these samples.

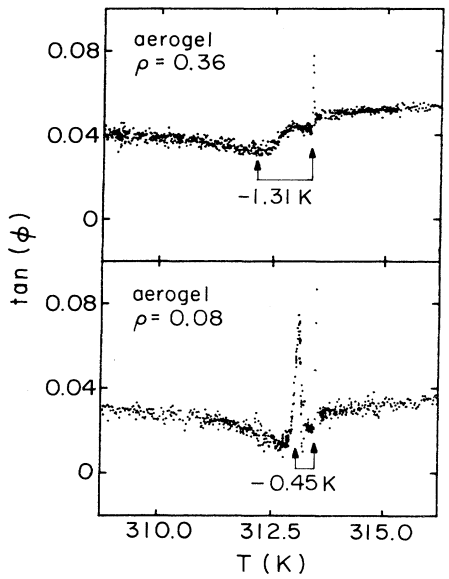

FIG. 3. Variation of the phase shift ϕ with temperature near the N-I transition of 8CB in two aerogels (see text). The extremely sharp high-temperature spike in both panels is due to N-I coexistence at the first-order transition in the trace amounts of bulk 8CB on the surface of the gel. A similar peak in tanϕ for the $\rho=0.08$ aerogel indicates two-phase N-I coexistence and first-order character also occurs for 8CB in this gel.

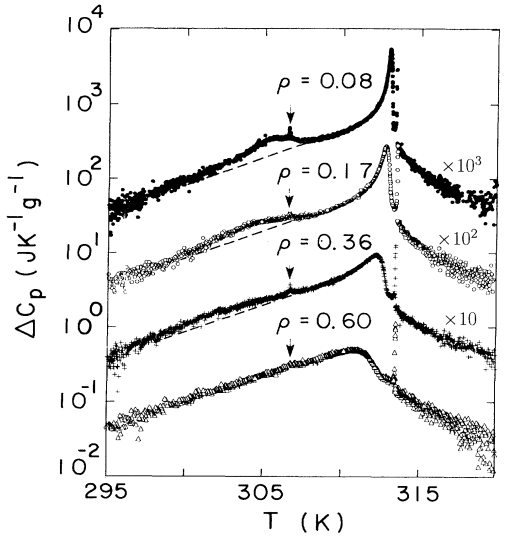

FIG. 4. Semilog plot of ΔC_p for four aerogels. As indicated, the data for three of the gels have been shifted vertically by factors of 10. The low-temperature N-I wings expected in the absence of a N–Sm-A transition are indicated by the dashed lines. The sharp N–Sm-A surface spikes are marked by arrows. The difference T_c(aerogel)$-T_c$(spike) in the two N–Sm-A peak positions is -0.98 ± 0.05 K for $\rho=0.08$, -1.62 ± 0.10 K for $\rho=0.17$, and -2.7 ± 0.2 K for $\rho=0.36$.

Since the N–Sm-A peak for 8CB in an aerogel is appreciably smaller and more smeared out than the N-I peak, it is convenient to display our ΔC_p data in a semilog plot, as shown in Fig. 4. This representation allows both the large N-I peak and the less distinct N–Sm-A peak to be compared. The quantity $\Delta C_p(N\text{–Sm-}A)$ corresponds to the excess heat capacity above the dashed line drawn for the low temperature wing of the N-I peak. Note in Fig. 4 that the surface N-I and N–Sm-A spikes occur at essentially the same temperature for all aerogels: 313.48 ± 0.05 K for the N-I spike and 306.65 ± 0.06 K for the N–Sm-A spike. There is also good agreement in ΔC_p values in the N-I wings, except of course in the vicinity of the N–Sm-A transition, as demonstrated in Figs. 5 and 6.

Figure 5 shows a superposition of $\Delta C_p(N\text{-}I)$ peaks in the vicinity of the N-I transition temperature. Figure 6, which covers a wide temperature range, shows on a greatly expanded heat capacity scale the ΔC_p behavior for the N-I wings and in the N–Sm-A transition region. The dashed curve represents the $\Delta C_p(N\text{-}I)$ variation that would be expected in the absence of a N–Sm-A transition. It was obtained from ΔC_p data below T_{NI} by excluding the N–Sm-A region (i.e., $-15<\Delta T<-4$ K) and fitting the remaining data with a power-law expression [26]. All three $\Delta C_p(N\text{-}I)$ curves are well represented by the dashed curve in Fig. 6 and these low-temperature N-I wings also correspond to the dashed lines shown in Fig. 4.

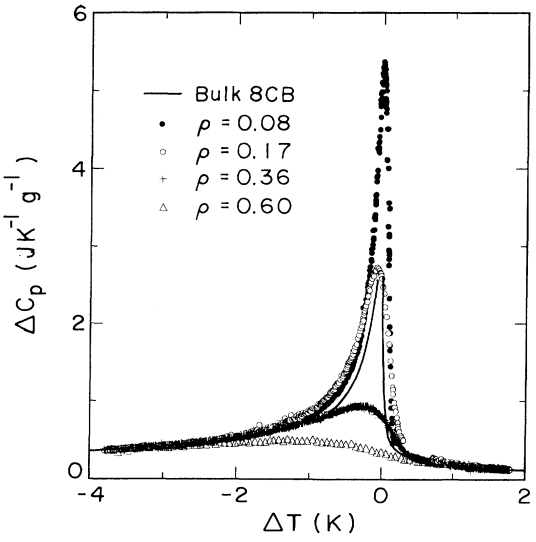

FIG. 5. Excess heat capacity $\Delta C_p(N\text{-}I)$ associated with the N-I transition for bulk 8CB [22] and for 8CB in four aerogels. The sharp surface spikes have been omitted from the aerogel data as have the artificially high C_p(coex) points due to first-order two-phase coexistence in the bulk 8CB. ΔT represents $T-T_{NI}^{\text{bulk}}$ for bulk 8CB and $T-T_0$ for the aerogel samples with $T_0=313.03$ K for $\rho=0.08$, $T_0=312.77$ K for $\rho=0.17$, $T_0=312.50$ K for $\rho=0.36$, and $T_0=312.03$ K for $\rho=0.60$.

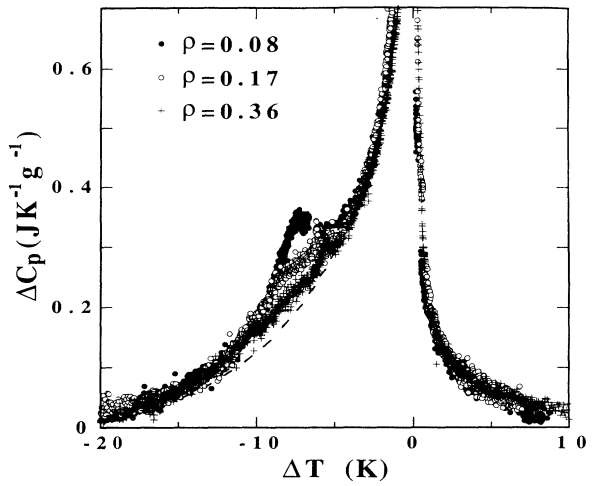

FIG. 6. Overlay of ΔC_p data for aerogels with $\rho=0.08$, 0.17, and 0.36 $g\,cm^{-3}$ over an expanded temperature range. $\Delta T=T-T_0$ with T_0 values the same as those used in Fig. 5. The dashed curve represents the low-temperature N-I wing expected in the absence of a N–Sm-A transition (see text).

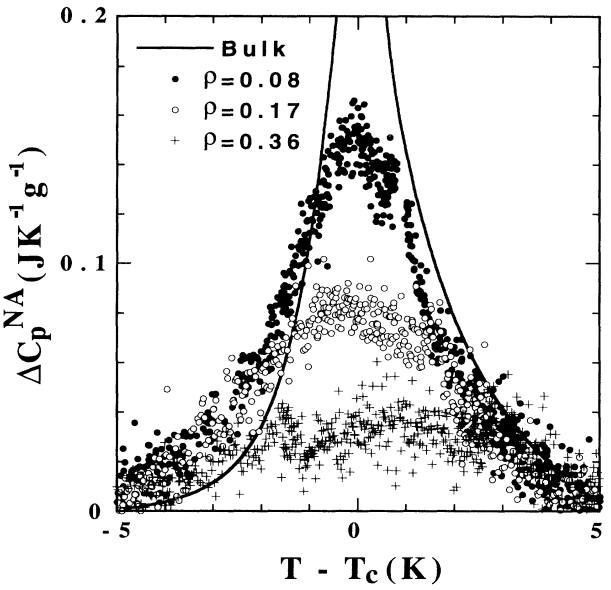

FIG. 7. Excess heat capacity $\Delta C_p(N\text{–Sm-}A)$ associated with the N–Sm-A transition for 8CB in three aerogels; the T_c values are given in Table II. The comparable quantity for bulk 8CB [21] is shown by the smooth curve.

Once the N-I base line behavior has been established, we can obtain the $\Delta C_p(N\text{–Sm-}A)$ excess associated with the N–Sm-A transition for 8CB in an aerogel from

$$\Delta C_p(N\text{–Sm-}A)=\Delta C_p-\Delta C_p(N\text{-}I)\ , \tag{3}$$

where ΔC_p is the total excess heat capacity obtained from Eq. (2) and $\Delta C_p(N\text{-}I)$ is taken to be the dashed curve in Fig. 6. The resulting $\Delta C_p(N\text{–Sm-}A)$ values for three of the aerogels are shown in Fig. 7. In the case of the $\rho=0.60$ aerogel, we could not unambiguously establish the presence of a N–Sm-A transition from our C_p data. The $p=0.36$ sample exhibits a definite $\Delta C_p(N\text{–Sm-}A)$ excess, but even in this case it is difficult to define the position of the maximum.

III. ANALYSIS AND DISCUSSION

The essential results of our calorimetric measurements are given in Figs. 5 and 7, which show the behavior of $\Delta C_p(N\text{-}I)$ and $\Delta C_p(N\text{–Sm}A)$, respectively. The apparent transition temperatures T_{NI} and T_{NA} for 8CB in an aerogel have been taken to be the temperatures at the maxima for ΔC_p. These values are given in Table II together with the shift ΔT_c in the transition temperature with respect to that for bulk 8CB, the maximum value of ΔC_p, and the integrated enthalpies defined by

$$\delta H_{NI}=\int \Delta C_p(N\text{-}I)dT\ ,\quad \delta H_{NA}=\int \Delta C_p(N\text{–Sm-}A)dT. \tag{4}$$

The liquid crystal transition temperatures and integrated enthalpies are plotted as a function of aerogel density in Figs. 8 and 9. The enthalpy values for bulk 8CB [22] are given for comparison. In the case of the first-order N-I transition in bulk 8CB, the quantity shown is the sum of the integrated area of the pretransitional wings and the discontinuous latent heat: $\delta H+\Delta H=5.58+2.10=7.68$ $J\,g^{-1}$.

The present 8CB-aerogel results for $\rho=0.36$ are in good qualitative agreement with those reported in Ref. [6]. The shifts in T_{NI} are comparable (-1.24 K in Ref.

TABLE II. Position and magnitude of $\Delta C_p(N\text{-}I)$ and $\Delta C_p(N\text{–Sm-}A)$ peaks for 8CB in aerogels of density ρ. T_c denotes the temperature of ΔC_p(max) and $\Delta T_c=T_c$(aerogel)$-T_c$(bulk) is the shift in C_p peak position with respect to bulk 8CB; $h\equiv\Delta C_p$(max) and δH is the integrated enthalpy.

Transition	ρ ($g\,cm^{-3}$)	T_c (K)	ΔT_c (K)	h ($J\,K^{-1}\,g^{-1}$)	δH ($J\,g^{-1}$)
N-I	0.08	313.03	−0.45±0.04	5.36±0.2	6.52±0.05
	0.17	312.76	−0.72±0.05	2.73±0.1	6.28±0.05
	0.36	312.17	−1.31±0.05	0.94±0.1	5.23±0.05
	0.60	310.90	−2.58±0.20	0.49±0.05	4.60±0.05
N–Sm-A	0.08	305.67	−0.98±0.05	0.153±0.01	0.60±0.05
	0.17	305.03	−1.62±0.10	0.086±0.01	0.43±0.05
	0.36	304.0	−2.7±0.2	0.035±0.01	0.23±0.05

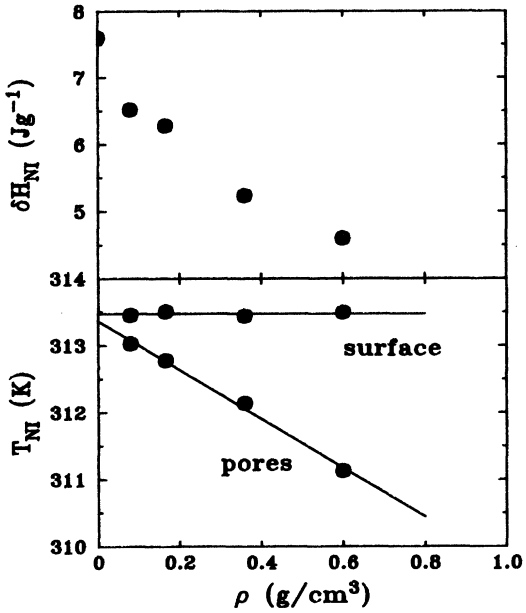

FIG. 8. $\Delta C_p(N\text{-}I)$ peak positions and N-I enthalpy for 8CB in aerogels of density ρ. The temperatures of the very sharp first-order spikes due to excess bulk 8CB on the surface are also shown for comparison.

6 and -1.31 K from Table II), but the magnitudes of the $\Delta C_p(N\text{-}I)$ peak differ. The integrated area δH_{NI} was estimated to be 3.6 ± 0.45 J g^{-1} in [6] compared to the present value of 5.23 J g^{-1}. We have no explanation for this difference in enthalpies, but it should be noted that the 8CB used in Ref. [6] was from a different batch and exhibited transition temperatures ~ 0.7 K lower than those for the present sample. The results reported here for the $\rho=0.36$ sample are reproducible on several runs and agree well with the overall pattern of $\Delta C_p(N\text{-}I)$ behavior as a function of aerogel density. Thus they are considered more reliable than those reported in Ref. [6].

It is obvious that the N-I and N–Sm-A transitions for 8CB are significantly modified when this liquid crystal is in the void space of a low-density aerogel. Although the shift in transition temperature and the diminution in the magnitude of ΔC_p are substantially greater for the N–Sm-A transition than for the N-I transition, the heat capacity peaks associated with both these transitions are sensitive to the density and therefore to the effective size of the void spaces in the aerogel. Thus it is of interest to assume that each aerogel can be characterized by a single parameter given by the average pore chord L and consider the dependence on L of $\Delta T_c \equiv T_c(L) - T_c(\infty)$ and $h \equiv \Delta C_p^{\max}(L)$. The quantity $T_c(\infty)$ is the bulk transition temperature and $T_c(L)$ is that for liquid crystal in an aerogel with pore chord L. The dependences of ΔT_c and h on L for the N-I and the N–Sm-A transition are shown in Figs. 10 and 11, where it is understood that the latent heat at the bulk N-I transition can be taken to be equivalent to a δ function for ΔC_p. In spite of the size of the errors bars for the aerogels with $\rho \geq 0.36$, there is a clear contrast between the behavior of these two transitions. Figure 10 shows that $|\Delta T_{NI}| \propto L^{-1}$ and $|\Delta T_{NA}| \propto L^{-0.72}$ when a power-law form is assumed; Fig. 11 yields $h \propto L^{1.33}$ for the N-I transition and $h \propto L^{1.0}$ for the N–Sm-A transition. This L dependence of ΔT_c is consistent with Figs. 8 and 9 since one finds empirically that the variation of $1/L$ with ρ is close to linear for these aerogels. A least-squares fit to the data in Table I yields $1/L = (1.55\times10^{-3})\rho$, where L is in Å and ρ in g cm^{-3}. This density dependence for L implies that these aerogels consist of fractal networks with a volume-fractal dimension $D \approx 2$, as mentioned previously.

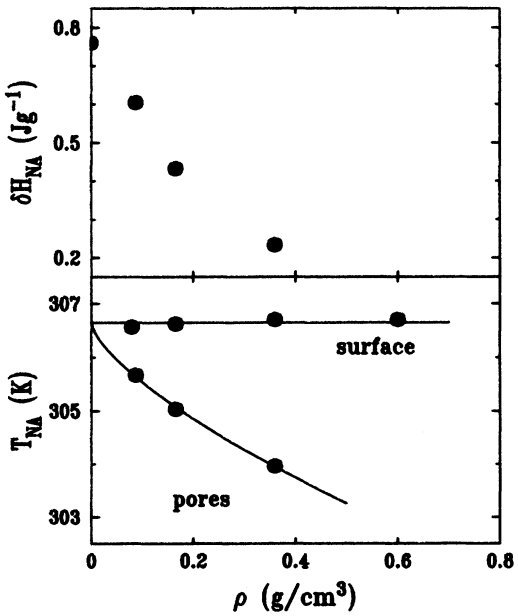

FIG. 9. $\Delta C_p(N\text{–Sm-}A)$ peak positions and N–Sm-A enthalpy for 8CB in three aerogels. The temperatures of the small but sharp spikes associated with the second-order N–Sm-A transition in excess bulk 8CB on the surface are shown for comparison.

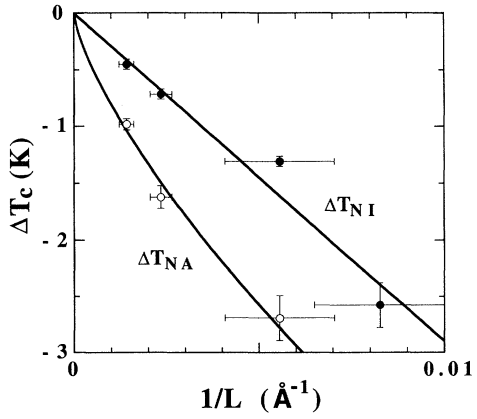

FIG. 10. Dependence on the shift in transition temperature $\Delta T_c = T_c(L) - T_c(\infty)$ on $1/L$ for N-I (●) and N–Sm-A (○) transitions, where L is the average pore chord for an aerogel. The quantity $1/L$ is roughly proportional to the model parameter p that specifies the fraction of 8CB molecules orientationally pinned by the silica surface (see text).

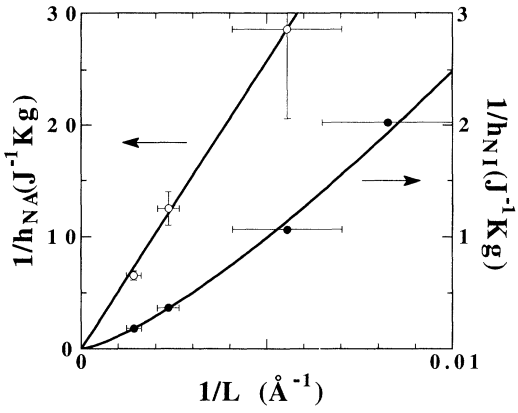

FIG. 11. Dependence of $h \equiv \Delta C_p(\max)$ on $1/L$ for N-I (●) and N–Sm-A (○) transitions.

One explanation to consider is the possibility that the behavior shown in Figs. 10 and 11 is due to finite size effects. For a bulk transition that is second order, finite-size scaling predicts $\Delta T_c \propto L^{-1/\nu}$ and $h \propto L^{\alpha/\nu}$, where ν is the critical exponent for the correlation length [27,28]. For a first-order bulk transition, it has been predicted that $h \propto L^d$, where d is the spatial dimension [29]. However, there are several arguments against finite size being the dominant influence on the behavior of 8CB in these aerogels. First, there is the interconnectivity of the aerogel void space (recall that the aerogel is filled by capillary action), which means that order can be correlated over large distances. Second, the empirical powers 0.72 and 1.0 do not correspond to $1/\nu$, and α/ν for the N–Sm-A transition. For bulk 8CB, $\alpha=0.31$, $\nu_\parallel=0.67$, and $\bar{\nu}=(\nu_\parallel+2\nu_\perp)/3=0.56$ for the N–Sm-A transition [22,30]. Thus $1/\nu=1.67-1.79$ and $\alpha/\nu=0.46-0.55$. Also $h \propto L^{1.33}$ does not agree with $h \propto L^d$ for the N-I transition. Third, finite-size scaling predicts that a set of excess heat capacity curves $\Delta C_p(L)$ as a function of $\Delta T = T - T_c(L)$ should nest under each other with $\Delta C_p(L)$ values being the same for all L when ΔT is large. Deviations of $\Delta C_p(L)$ from the bulk $\Delta C_p(\infty)$ curve will first occur at a temperature difference $|\Delta T^*|$ where the correlation length ξ is comparable to the sample size L. Figure 7 shows that the ΔC_p (N–Sm-A) data for three aerogel samples nest in a reasonable looking way but the wings of these $\Delta C_p(L)$ curves do not match the $\Delta C_p(\infty)$ bulk curve, especially for $T < T_c$. Even for $T > T_c$, the deviation of each aerogel curve from the high-temperature $\Delta C_p(\infty)$ wing occurs at a much larger ΔT value than expected from the known behavior of $\xi_\parallel$ in bulk 8CB. For bulk 8CB in the nematic phase, where the longitudinal correlation length $\xi_\parallel$ is given by $\xi_\parallel$ (Å)$=208\Delta T^{-0.67}$ [30], one would expect $\Delta T^* \simeq 0.16$ K when $\xi_\parallel = L = 700$ Å for the $\rho=0.08$ aerogel, $\Delta T^* \simeq 0.34$ K when $\xi_\parallel = L = 430$ Å for the $\rho=0.17$ aerogel, and $\Delta T^* \simeq 1.24$ K when $\xi_\parallel = L = 180$ Å for the $\rho=0.36$ aerogel. Even if one ignored the bulk 8CB curve in Fig. 7 and assumed that the $\rho=0.08$ aerogel data corresponded to bulk behavior for $|\Delta T| = |T - T_c| > 1$ K one cannot match finite-size predictions since $\rho=0.17$ and 0.36 aerogel data deviate at $|\Delta T| \simeq 1.8$ and $|\Delta T| \simeq 3$ K, respectively, values that are far larger than the $\Delta T^* = 0.34$ and 1.24 K estimates.

In the case of the N-I transition, Fig. 5 shows that the $\Delta C_p(L)$ wings for the aerogel samples do agree with $\Delta C_p(\infty)$ for bulk 8CB when $\Delta T = T - T_0 \geq +0.5$ K and $\Delta T \leq -2$ K. However, there is the complication that the bulk transition is first order. For the $\rho=0.08$ and 0.17 aerogels, there is a smeared first-order transition with N-I two-phase coexistence over the range $-0.22 < \Delta T < +0.10$ K and $\Delta C_p(L)$ values greater than $\Delta C_p(\infty)$ over the considerably wider range of $-1.2 < \Delta T < +0.35$ K. For the $\rho=0.36$ and 0.60 aerogels, $\Delta C_p(L) < \Delta C_p(\infty)$ for all ΔT, but the T_0 value used to overlay data in Fig. 5 is not equal to the peak temperature T_c.

It is of interest to compare the presently observed C_p results with those from a study of 8CB in Anopore (alumina) membranes with a quite regular array of nearly cylindrical pores 2000 Å in diameter and 60 μm in length [9]. In untreated Anopore membranes, surface interactions align molecules such that the director is parallel to the pore axis. In membranes treated with lecithin, the director orientations are normal to the surface. Our C_p data are qualitatively more similar to those for 8CB in untreated (axial) Anopore than in the lecithin-treated (radial) Anopore. In particular, the radial N-I peak is appreciably broadened on the high-temperature side and has a symmetric profile, unlike the axial N-I peak in Anopore or our aerogel N-I peaks which exhibit an asymmetric shape similar to bulk 8CB. There are, however, considerable quantitative differences between the aerogel results and those in Anopore. For the axial 8CB in Anopore, the T_c shifts and $h \equiv \Delta C_p(\max)$ values are $\Delta T_c = -0.69$ K, $h = 1.55$ J K^{-1} g^{-1} for the N-I transition and $\Delta T_c = -0.90$ K, $h = 0.27$ J K^{-1} g^{-1} for the N–Sm-A transition. For the radial 8CB in Anopore, the corresponding values are $\Delta T_c = -1.34$ K, $h = 1.03$ J K^{-1} g^{-1} for N-I and $\Delta T_c = -0.71$ K, $h = 0.11$ J K^{-1} g^{-1} for N–Sm-A. In contrast to these large ΔT_c values observed for 8CB in Anopore, the smooth curves in Fig. 10 predict $\Delta T_{NI} = -0.15$ K and $\Delta T_{NA} = -0.46$ K for $L = 2000$ Å in an aerogel.

Thus we believe the liquid crystal-aerogel results reflect primarily random-field effects as proposed theoretically [12,13] rather than surface effects or the usual finite-size effects. This view is supported by calorimetric results for the homolog 7CB in a Vycor porous glass with 3D randomly connected pore segments of length ~300 Å and relatively uniform diameter ~70 Å [10]. In this case the ΔT_c shift associated with the N-I transition is approximately −3.5 K, which compares fairly well with the value −4.1 K obtained by extrapolation of the ΔT_{NI} line in Fig. 10 to $L = 70$ Å.

Unfortunately, the theory of the phase behavior of liquid crystals in random porous media is not yet well developed. Gingras [12] has argued that the effect of a quenched random network on the nematic order leads to a random-field description of the N-I transition rather

than a spin-glass description. He further predicts that weak disorder will destroy the N–Sm-A transition, converting it into a spin-glass-like transition in the same universality class as the vortex-glass transition in disordered type-II superconductors. Maritan *et al.* [13] have developed a simplified model for the N-I transition in a porous medium and have carried out an analysis of this model using mean-field theory and Monte Carlo simulations. A key variable in this theory is p, the fraction of sites having a large quenched random local field. The model predicts a threshold value $p_{\max}$. For $0 \leq p \leq p_{\max}$, a first-order phase transition to a long-ranged-ordered nematic phase will occur at a progressively lower temperature $T(0) \geq T(p) \geq T(p_{\max}) = 0$. For $p > p_{\max}$, there is no thermodynamic phase transition, but the response functions such as ΔC_p still exhibit broad weak maxima centered at temperatures below $T(0)$. The general N-I behavior for liquid crystals in a porous medium predicted in this Maritan model is also obtained in a very recent mean-field analysis of the random anisotropy nematic model [31].

In the context of the Maritan model, we can approximate the parameter p as lying somewhere between $wS/\phi_p = 4w/L$ and $1-\phi_p+wS = (4w+d_s)/(L+d_s)$, where $S = 4/d = 4/(L+d_s)$ is the solid area per unit volume of aerogel, $\phi_p = L/d$, d_s is the solid chord [17], and w is the thickness of a layer of liquid crystal molecule in contact with the silica interface. If we assume that w is constant, the fraction p of 8CB molecules directly influenced by the silica surface (i.e., the strong random local field) is proportional to $1/L$ in the first limiting case and still varies like $1/L$ for large L in the second limiting case. Thus the plots of ΔT_c and $1/h$ in Figs. 10 and 11 can be interpreted as giving roughly the dependence of these quantities on p. On this basis we propose that $p_{\max}$ for the N-I transition is achieved for an aerogel with a density $0.17 < \rho < 0.36$. Unlike the result from the simplified theoretical model, $T(p_{\max}) \neq 0$. Instead there is a smooth variation of the quantity $T_c(N\text{-}I)$ with p from $p = 0$ to $p > p_{\max}$, where T_c has been chosen as the temperature of the ΔC_p maximum. Thus T_c denotes the location of the first-order N-I transition for $p < p_{\max}$ and the location of the rounded maximum in the thermal response function when $p > p_{\max}$. The experimental situation here is somewhat analogous to quenched random field effects on the orientational transition in mixed cyanide crystals [32]. In that case, a weakly first-order transition line terminates at $T(p_{\max}) \approx p_{\max} T(0)$, where $p_{\max}$ varies from 0.25 to 0.45 for different mixed crystals.

It should be noted that a synchrotron x-ray study has been carried out on the N–Sm-A transition of 8CB in exactly the same four aerogels used in the present work [33]. Scattering at the smectic wave vector $q \simeq 0.2$ Å^{-1} can be represented by the sum of two Lorentzian—a broad weak Lorentzian associated with small smectic domains and a narrower Lorentzian associated with larger domains. The intensity of the broad Lorentzian goes through a maximum at a temperature near that of the ΔC_p maximum, while the narrower Lorentzian evolves (grows in intensity and becomes progressively narrower) on cooling over a 20 K range below the $\Delta C_p(N\text{–Sm-}A)$ peak position. This suggests domain growth leading to Sm-A domain sizes greater than L for temperatures well below the N–Sm-A "transition" T_c as given by calorimetry. A detailed report of this x-ray work [33] will include a comparison of the temperature range for the evolution of Sm-A scattering and that for the excess heat capacity $\Delta C_p(N\text{–Sm-}A)$ shown in Fig. 7.

IV. CONCLUSION

When the liquid crystal 8CB is placed in a high-porosity silica aerogel, the weakly first-order N-I and second-order N–Sm-A phase transitions are substantially modified. A calorimetric study of the excess heat capacities $\Delta C_p(N\text{-}I)$ and $\Delta C_p(N\text{–Sm-}A)$ as a function of aerogel density shows that the N–Sm-A transition is especially sensitive to the random field effects of the silica network. The $\Delta C_p(N\text{-}I)$ data show that the two-phase coexistence of N and I at a very weakly first-order transition persists for aerogels with densities $\rho = 0.08$ and 0.17 g cm^{-3}, but is not detected for aerogels with $\rho = 0.36$ and 0.60. The temperature and magnitude of $\Delta C_p^{\max}$ vary systematically with the density ρ or average pore chord L, but these changes cannot be well represented as finite-size effects. It appears that quenched random field effects are dominant, as proposed theoretically [12,13,31]. In this case the fraction p of liquid crystal molecules orientationally frozen by the silica network should be roughly proportional to $1/L$.

ACKNOWLEDGMENTS

The authors wish to thank L. Hrubesh for providing the aerogels with density $\rho = 0.36$ and 0.60 g cm^{-3} and to thank N. A. Clark and A. G. Rappaport for stimulating discussions. This work was supported in part by National Science Foundation Grants Nos. DMR 90-22933 and DMR 93-11853. The work carried out at Sandia National Laboratories was supported by the U.S. Department of Energy Office of Basic Energy Sciences under Contract No. DE-AC04-94AL85000.

[1] A. P. Y. Wong and M. H. W. Chan, Phys. Rev. Lett. **65**, 2567 (1990).

[2] A. P. Y. Wong, S. B. Kim, W. I. Goldburg, and M. H. W. Chan, Phys. Rev. Lett. **70**, 954 (1993).

[3] B. J. Frisken and D. S. Cannell, Phys. Rev. Lett. **69**, 632 (1992), and references cited therein.

[4] N. Mulders, R. Mehrotra, L. S. Goldner, and G. Ahlers, Phys. Rev. Lett. **67**, 695 (1991), and references cited therein.

[5] S. B. Kim, J. Ma, and M. H. W. Chan, Phys. Rev. Lett. **71**, 2268 (1993).

[6] T. Bellini, N. A. Clark, C. D. Muzny, L. Wu, C. W. Gar-

land, D. W. Schaefer, and B. J. Oliver, Phys. Rev. Lett. **69**, 788 (1992).

[7] X-l. Wu, W. I. Goldburg, M. X. Liu, and J. Z. Xue, Phys. Rev. Lett. **69**, 470 (1992); T. Bellini, N. A. Clark, and D. W. Schaefer, Phys. Rev. Lett. (to be published).

[8] N. A. Clark, T. Bellini, R. M. Malzbender, B. N. Thomas, A. G. Rappaport, C. D. Muzny, D. W. Schaefer, and L. Hrubesh, Phys. Rev. Lett. **71**, 3505 (1993).

[9] G. S. Iannacchione and D. Finotello, Phys. Rev. Lett. **69**, 2094 (1992), and references therein; Liq. Cryst. **14**, 1135 (1993).

[10] G. S. Iannacchione, G. P. Crawford, S. Zumar, J. W. Doane, and D. Finotello, Phys. Rev. Lett. **71**, 2595 (1993).

[11] M. D. Dadmun and M. Muthukumar, J. Chem. Phys. **98**, 4850 (1993).

[12] M. J. P. Gingras (unpublished).

[13] A. Maritan, M. Cieplak, T. Bellini, and J. R. Banavar, Phys. Rev. Lett. **72**, 4113 (1994).

[14] D. W. Schaefer and K. D. Keefer, Phys. Rev. Lett. **56**, 2199 (1986).

[15] F. Ferri, B. J. Frisken, and D. S. Cannell, Phys. Rev. Lett. **67**, 3626 (1991).

[16] R. Vacher, T. Woignier, J. Pelous, and E. Courtens, Phys. Rev. B **37**, 6500 (1988).

[17] D. W. Schaefer, Mat. Res. Soc. Bull. **14-4**, 49 (1994); see also a general discussion in A. Emmerling and J. Fricke, J. Non-Cryst. Solids **145**, 113 (1992).

[18] R. G. Priest and T. C. Lubensky, Phys. Rev. B **13**, 4159 (1976).

[19] P. A. Lebwohl and G. Lasher, Phys. Rev. A **6**, 426 (1972); **7**, 2222 (1973).

[20] W. Maier and A. Saupe, Z. Naturforsh. A **14**, 852 (1959); **15**, 287 (1960).

[21] G. B. Kasting, C. W. Garland, and K. Lushington, J. Phys. (Paris) **41**, 879 (1980).

[22] J. Thoen, H. Marynissen, and W. VanDael, Phys. Rev. A **26**, 2886 (1982).

[23] T. M. Tillotson and L. W. Hrubesh, J. Non-Cryst. Solids **145**, 44 (1992).

[24] C. W. Garland, Thermochim. Acta **88**, 127 (1985), and references cited therein; K. J. Stine, Ph.D. thesis, Massachusetts Institute of Technology, 1988.

[25] K. Ema, G. Nounesis, C. W. Garland, and R. Shashidhar, Phys. Rev. A **39**, 2599 (1989); X. Wen, C. W. Garland, and M. D. Wand, *ibid.* **42**, 6087 (1990); K. J. Stine and C. W. Garland, Mol. Cryst. Liq. Cryst. **188**, 91 (1990).

[26] The expression $\Delta C_p(N\text{-}I)=At^{-\alpha}(1+Dt^{0.5})$, where $t=(T_{NI}-T)/T_{NI}$, was used. The empirical effective exponent α of ~ 0.35 is in reasonable agreement with α values obtained from fits to $\Delta C_p(N\text{-}I)$ data for bulk 8CB in Ref. [22]. Such power-law fits provide a useful interpolation scheme, although the α values do not represent asymptotic *N-I* critical-fluctuation behavior. See J. Thoen, in *Phase Transitions in Liquid Crystals,* Vol. 290 of *NATO Advanced Study Institute, Series B: Physics,* edited by S. Martellucci and A. N. Chester (Plenum, New York, 1992), Chap. 10.

[27] M. E. Fisher and A. E. Ferdinand, Phys. Rev. Lett. **19**, 169 (1967); M. E. Fisher and M. N. Barber, *ibid.* **28**, 1516 (1972).

[28] W. Hahn and V. Dohm, Phys. Rev. Lett. **61**, 1368 (1988), and references cited therein.

[29] M. E. Fisher and A. N. Berker, Phys. Rev. B **26**, 2507 (1982).

[30] D. Davidov, C. R. Safinya, M. Kaplan, S. S. Dana, R. Schaetzing, R. J. Birgeneau, and J. D. Litster, Phys. Rev. B **19**, 1657 (1979).

[31] D. J. Cleaver, S. Kralj, T. J. Sluckin, and M. P. Allen (unpublished).

[32] J. O. Fossum, A. Wells, and C. W. Garland, Phys. Rev. B **38**, 412 (1988); J. O. Fossum and C. W. Garland, J. Chem. Phys. **89**, 7441 (1988).

[33] A. G. Rappaport, B. N. Thomas, N. A. Clark, T. G. Bellini, D. W. Schaefer, and L. Hrubesh (unpublished).